• Original Paper •

Comparison of Ozone Fluxes over a Maize Field Measured with Gradient Methods and the Eddy Covariance Technique

Zhilin ZHU[*1,2], Xinzhai TANG[1], and Fenghua ZHAO[1]

[1]*Key Laboratory of Ecosystem Network Observation and Modeling*, *Institute of Geographic Sciences and Natural Resources Research*, *Chinese Academy of Sciences*, *Beijing* 100101, *China*
[2]*College of Resources and Environment*, *University of Chinese Academy of Sciences*, *Beijing* 100049, *China*

ABSTRACT

Ozone (O_3) fluxes were measured over a maize field using the eddy covariance (EC) technique and gradient methods. The main objective was to evaluate the performance of the gradient methods for measuring the O_3 flux by comparing them with the EC O_3 flux. In this study, turbulent exchange coefficients (K) calculated with three methods were compared. These methods were the aerodynamic gradient (AG) method (in which K is calculated by using wind speed and temperature gradients), the aerodynamic gradient combined with EC (AGEC) method, in which the friction velocity and other variables are based on EC measurements, and the modified Bowen ratio using the EC sensible heat flux and temperature gradient (MBR) method. Meanwhile, the effects of the measurement and calculation methods of the O_3 concentration gradient were analyzed. The results showed that: (1) on average, the transfer coefficient computed by the MBR method was 40% lower, and the coefficient determined with the AG method was 25% higher, than that determined with the AGEC method. (2) The gradient method's O_3 fluxes with the MBR, AGEC, and AG methods were 30.4% lower, 11.7% higher, and 45.6% higher than the EC O_3 flux, respectively. (3) The effect of asynchronous O_3 concentration measurements on the O_3 gradient must be eliminated when using one analyzer to cyclically measure two-level O_3 concentrations. The accuracy of gradient methods for O_3 flux is related to the exchange coefficient calculation method, and its precision mainly depends on the quality of the O_3 gradient.

Key words: ozone flux, eddy covariance, gradient method, ozone gradient, eddy diffusivity

Article Highlights:

• Three methods for calculating eddy diffusivities were compared, and the diffusivity calculated with EC data was the optimal method.
• There were some differences in O_3 fluxes measured with gradient methods and the EC technique.
• The accuracies of gradient methods are related to eddy diffusivity, and the uncertainties depend on the O_3 gradient quality.
• Ways for reducing the uncertainty of the O_3 gradient are discussed.

---

1. Introduction

Although only approximately 10% of the total O_3 is in the troposphere (Krzyscin et al., 2007), as a secondary pollutant near the ground, tropospheric O_3 is known to have negative effects on human health, vegetation, and ecosystems (Massman, 2004; Cape, 2008). In China, rapid industrialization and urbanization have been resulting in increases in the atmospheric O_3 concentration, threatening human health and crop yields (Feng et al., 2015; Fu et al., 2019).

To quantitatively assess the effects of O_3 on vegetation and ecosystems, several O_3 concentration–based and stomatal flux–based indices have been proposed and applied in recent decades (Musselman et al., 2006; Karlsson et al., 2007). Considering the amount of O_3 entering vegetation stomata, some studies have shown that the effect of O_3 on vegetation is more closely related to the stomatal O_3 flux (Paoletti and Manning, 2007; Pleijel et al., 2007; Mills et al., 2011). Measuring the O_3 flux over ecosystems is an important step

---

* Corresponding author: Zhilin ZHU
  Email: zhuzl@igsnrr.ac.cn

for calculating flux-based indices. In addition, the O_3 flux can also facilitate our understanding of O_3 deposition processes.

Currently, two main micrometeorological techniques, the eddy covariance (EC) method and gradient method, are applied to measure the O_3 flux (Grünhage et al., 2000). Although there are some errors and uncertainties in the EC method (Massman and Lee, 2002), it is considered the best direct flux measuring method and is widely used for carbon dioxide (CO_2) and water flux measurements (Baldocchi, 2003). Nevertheless, the EC approach to O_3 flux measurement is currently not very popular, as the fast-response O_3 analyzers employed for the task do not perform as well as CO_2 and H_2O gas analyzers (Muller et al., 2010; Zahn et al., 2012). For example, an O_3 analyzer's sensitivity is variable owing to the consumption of O_3-sensitive dye and changes in environmental conditions (Güsten et al., 1992). It needs a slow analyzer to simultaneously calibrate it nearby, which could result in different fluxes when using different calibration methods (Zhu et al., 2015). The EC technique avoids measuring the O_3 gradient, which is considered to be the main source of uncertainty in O_3 fluxes measured with gradient methods, resulting in the EC-measured O_3 flux being considered more reliable (Muller et al., 2009; Loubet et al., 2013).

Although the EC method for O_3 flux measurements is becoming increasingly popular at present, the gradient method is still used for measuring O_3 flux and has been improved (Muller et al., 2009; Bocquet et al., 2011; Mayer et al., 2011; Loubet et al., 2013). For the traditional gradient method, the largest uncertainty comes from the error of O_3 concentration differences or a small gradient that is often the same order of magnitude as the analyzer's precision. Recently, Wu et al. (2015) proposed a modified micrometeorological gradient method for estimating ozone flux over a forest canopy, in which the O_3 gradients were calculated from the O_3 concentrations between a level above and a level below the canopy top. The advantage is that the relatively large gradients between these levels make this method more stable. Compared to other traditional gradient methods, it was the closest in magnitude to the EC measurements.

The gradient method for determining O_3 flux is the product of eddy transfer diffusivity and the O_3 concentration difference (gradient) at two or more heights. The O_3 gradient can be measured directly with analyzers, while the eddy transfer diffusivity is usually obtained by measuring other variables in the context of Monin–Obukhov similarity theory (MOST), i.e., the eddy transfer diffusivity for all scalars is assumed to be the same (Foken, 2006). Thus far, three methods for determining transfer diffusivity have been widely applied. The first method is based on momentum transfer diffusivity, which can be obtained by measuring the temperature and wind speed gradients (Baldocchi and Meyers, 1998; Bocquet et al., 2011). Although all variables in this method are easily measured with routine instruments, the high-precision gradients are difficult to obtain. The second

method uses the universal flux–gradient relationships. In this way, the transfer diffusivity could be determined without requiring temperature and wind speed measurements, if the friction velocity (u^*) and sensible heat flux (H) are measured by the EC technique (Loubet et al., 2013). This method overcomes the uncertainty in gradient measurements. The third method is the modified Bowen ratio (MBR) (Meyers et al., 1996; Walker et al., 2006; Mayer et al., 2011). This requires the measurement of another scalar flux (e.g., sensible heat, H_2O, CO_2) and its corresponding gradient over the same heights. The scalar flux can be measured with the EC technique, and its corresponding temperature or gas concentration gradient should be measured at the same heights. The inversely derived exchange coefficient of the scalar flux can be assumed to be equivalent to all scalar quantities in the ecosystem. Although fluxes can be measured with the EC method, it still requires the measurement of scalar gradients. Different methods might result in different transfer diffusivity values.

Although the gradient method is not as good as the EC technique, it has the advantage of being easy to apply broadly without an expensive EC system and fast-response O_3 analyzer. Nevertheless, investigators should first be familiar with the accuracy and precision of the gradient method. The main motivation of this study was to evaluate the performance of the gradient method by comparing its results with the EC O_3 flux. Compared with previous studies, the novelty of this study is the evaluation of the performance of three gradient methods for estimating O_3 flux by comparison with the EC technique. Meanwhile, the effects of the measurement and calculation methods of the O_3 concentration gradient were analyzed. The specific objectives of this study were to: (1) compare the difference and analyze the effects of diffusion coefficients calculated by different methods; (2) analyze the effects of different gradient calculation and measurement methods; and (3) evaluate the performance of the gradient method compared to the EC method for measuring the O_3 flux.

2. Materials and methods

2.1. *Site, instruments, and measurements*

Measurements were executed during daytime [0500–2000 LST(LST=UTC+8)] from 2 August to 28 September 2017 over a summer maize (*Zea mays*) field at the Yucheng Comprehensive Experimental Station, Chinese Academy of Sciences (36°57'N, 116°36'E; 36 m MSL). During the experiment periods, the maize was in the flourishing stage and its height was constant. The site was located in the Yellow River alluvial plain of the North China Plain, Shandong Province, China. The surface soil texture at the station was that of a silty loam with moderate salinity and alkalinity. The experimental site was fairly flat, and the fetch requirements for flux measurements were well satisfied within 200 m of the instrument locations. During the observation period, the mean crop height was 2.2 m.

Gradient measuring sensors and EC instruments were installed at two masts separated by a horizontal distance of approximately 3 m. For gradient measurements, all sensors or air sampling inlets were mounted at 4.70 m and 3.15 m. Two temperature and relative humidity sensors (HMP155A, Vaisala, Finland) were housed in special radiation shields. Wind speeds were measured with two 2D ultrasonic wind sensors (WMT700, Vaisala, Finland). The two-height O_3 concentrations were measured with a slow-response UV photometric O_3 analyzer (Model 205, 2B Technologies Inc., USA; hereafter referred to as M205). Its measurement precision is 1.0 ppb, with a resolution of 0.1 ppb. By using two solenoid valves, two-level air samples were cyclically (switching once per 5 min) drawn down into an analyzer with two separate inlet lines (PTFE Teflon) that were 5.5 m long with 4-mm inner diameters.

The EC O_3 flux was measured in combination with observations from the Chinese Terrestrial Ecosystem Flux Observational Research Network (or ChinaFLUX). The instrumentation included a 3D sonic anemometer (CSAT3, Campbell Scientific Inc., USA) and an open-path CO_2/H_2O gas analyzer (LI-7500, LI-COR, Nebraska, USA) for measuring sensible heat, latent heat, and CO_2 fluxes. The O_3 fluctuation (in mV) was measured with a closed-path fast-response O_3 analyzer that was cooperatively developed by Karlsruhe Institute of Technology and Enviscope GmbH (Germany) (Zahn et al., 2012; hereafter referred to as ENVI). Air was drawn down through a 4.5-m-long tube with a 4-mm inner diameter at a flow rate of 2.4 l min⁻¹ and passed over a small disc coated with O_3-sensitive dye. Its output signal (in mV) was positively correlated with the ambient O_3 concentration (Muller et al., 2010). Because of the continuous consumption of O_3-sensitive dye, we replaced the dye disc every 3–4 days, approximately. Radiation variables were also measured, including net radiation (CNR1, Kipp & Zonen, The Netherlands) and photosynthetically active radiation (LI-190SB, LI-COR, Nebraska, USA). All radiation and EC sensors were installed at a height of 3.5 m.

All gradient measurements were sampled with a frequency of 0.1 Hz, and the averages for every 5 min were recorded by a data-logger (CR3000). All high-frequency vector and scalar raw data were continuously sampled and stored using a SMARTFlux system (LI-COR, Nebraska, USA) with a frequency of 10 Hz.

2.2. *Gradient methods*

According to Fick's first law, the scalar flux in the constant-flux layer can be expressed as the product of the vertical concentration gradient ($\partial c/\partial z$) and eddy diffusivity (K_c) (Grünhage et al., 2000):

$$F_c = K_c \frac{\partial c}{\partial z} . \tag{1}$$

Usually, the gas concentration vertical gradient is obtained by directly measuring concentrations at two or more layers with one or more gas analyzer(s), while K_c is obtained from other measurements. Based on MOST, the

eddy diffusivity for O_3 can be assumed to be equal to the diffusivity for momentum, heat, water vapor, and trace gases. To assess the differences in the calculated K_c from using the different methods, three methods were selected in the present study, as briefly described below.

2.2.1. *Aerodynamic gradient method*

The first method, the aerodynamic gradient (AG) method, is based on the gradients of temperature, wind speed, and gas concentrations. As the two measurement heights of three variables are the same, the AG method O_3 flux can be calculated as (Bocquet et al., 2011):

$$F_{O_3\_AG} = \left(\frac{\kappa}{\ln[(z_2 - d)/(z_1 - d)]} \right)^2 \frac{\Delta \overline{U}}{\Phi_m \Phi_c} \Delta \overline{C}_{O_3} = K_{AG} \Delta \overline{C}_{O_3} , \tag{2}$$

where κ is the von Karman constant (0.4 in this study), d is the zero-plane displacement, estimated by the equation $d = 0.67 h_c$ (h_c is maize height), and z_2 and z_1 are the heights of the upper and lower sampling inlets and meteorological sensors, respectively. Φ_m and Φ_c are stability function of momentum and scalar, respectively. ΔU and ΔC_{O_3} are the mean gradients of the wind speed and O_3 concentration, respectively, the overbar denotes average, and K_{AG} is referred to as the exchange coefficient and is also called the transfer velocity (Meyers et al., 1996; Wolff et al., 2010). Note that the effect of the height difference (Δz) is subsumed in the exchange coefficient K with units of velocity (Meyers et al., 1996). The stability correction factors are calculated by:

$$\Phi_m \Phi_c = (1 - 5Ri)^{-2} \text{ (for } Ri > 0, \text{ stable conditions)} , \tag{3}$$

$$\Phi_m \Phi_c = (1 - 16Ri)^{-0.75} \text{ (for } Ri < 0, \text{ unstable conditions)} , \tag{4}$$

where the Richardson number (Ri) is estimated by:

$$Ri = \frac{g}{\overline{\theta}} \frac{(\Delta \overline{\theta}/\Delta z_\theta)}{(\Delta \overline{U}/\Delta z_u)^2} , \tag{5}$$

where g is the gravitational acceleration (9.8 m s⁻²), $\Delta \theta$ is the potential temperature gradient, and Δz_u and Δz_θ are the height differences in the wind speed and temperature, respectively. As the mean air pressure is very close to 1000 hPa, the potential temperature was replaced with the air temperature.

2.2.2. *AG method combined with EC measurements*

Since the EC system was employed in this experiment, the u^* and H can be obtained directly. Therefore, the K_c can be calculated using the universal flux–gradient relationships method (Businger et al., 1971). The O_3 flux calculated with this AG method with EC measurements (hereafter referred to as the AGEC method) can be written as (Rinne et al., 2000):

$$F_{O_3\_AGEC} = \cfrac{\kappa u^*}{\ln\left[\cfrac{(z_2-d)}{(z_1-d)}\right] - \Psi_h[(z_2-d)/L] + \Psi_h[(z_1-d)/L]}\Delta\overline{C}_{O_3}$$

$$= K_{AGEC}\Delta\overline{C}_{O_3} \qquad (6)$$

where the u^* and Obukhov length L are taken from the EC measurements. Ψ_h is the integrated stability correction function for heat calculated using the Businger–Dyer equations (Paulson, 1970; Businger et al., 1971).

2.2.3. MBR method

Based on the measurements of fluxes (momentum, sensible heat, and latent heat fluxes) and gradients (wind speed, temperature, and relative humidity), three MBR exchange coefficients could be calculated. In this study, the exchange coefficient with the MBR method was based only on the H and temperature gradient, and the O_3 flux for MBR was calculated as (Walker et al., 2006):

$$F_{O_3\_MBR} = (\overline{w'T'}/\Delta T)\Delta\overline{C}_{O_3} = K_{MBR}\Delta\overline{C}_{O_3} , \qquad (7)$$

where w is the vertical wind speed (m s^{-1}), $\overline{w'T'}$ is the kinematic heat flux (K m s^{-1}) measured by the EC method, the overbar denotes the time average, and the prime signs indicate the fluctuation of each variable. ΔT is the vertical gradient of air temperature (K). The ratio $\overline{w'T'}/\Delta T$ can be considered the exchange coefficient or the transfer velocity of the O_3 flux.

2.3. EC O_3 flux calculation

As the ENVI's output is a relative measure of the O_3 concentration, and its stability is affected by the consumption of O_3-sensitive dye and environmental conditions, it must simultaneously calibrate. In this study, the "ratio method" was used to calibrate the ENVI's signal-output (X), meaning that X (in mV) is proportional to the absolute ambient O_3 concentration over a 30-min period (Muller et al., 2010). Based on this assumption, the O_3 deposition velocity (V_d), defined as the O_3 flux divided by the O_3 concentration, can be calculated by:

$$V_d = \cfrac{\overline{w'X'}}{\overline{X}}, \qquad (8)$$

where the role of the minus sign in Eq. (8) is to maintain a positive V_d, because the O_3 flux is always directed downward (negative). The raw EC O_3 flux, $F_{O_3\_EC}$, can be given as:

$$F_{O_3\_EC} = -\overline{\rho}_{O_3}V_d = \frac{P}{T}\frac{M_{O_3}}{R}\frac{\overline{x_{O_3}}}{\overline{X}}\overline{w'X'} , \qquad (9)$$

where $\overline{\rho}_{O_3}$ is the mean O_3 density (nmol m^{-3}), $\overline{x_{O_3}}$ is the mean O_3 mixing ratio (ppb), P is air pressure, T is air temperature (K), R is the universal gas constant, and M_{O_3} is the molar mass of O_3.

In practice, the O_3 flux and other EC data were processed by EddyPro® software (LI-COR, NE, USA) with a series of corrections. The double rotation method was used

to correct the error due to non-level terrain (Wilczak et al., 2001). Ozone flux loss caused by time delay was corrected by the maximum covariance method (Moncrieff et al., 1997). The frequency response attenuation due to tubing was corrected using methods described by Ibrom et al. (2007). The Webb-Pearman-Leuning (WPL) correction (Webb et al., 1980) term only considered density variations caused by water vapor (Zhu et al., 2015).

3. Results and discussion

3.1. Comparison of the exchange coefficients from different methods

Exchange coefficients (K) are key factors for gradient method fluxes. Different methods of determining K result in different exchange coefficients. Figure 1 shows the mean diurnal variations of the transfer coefficients calculated by the three methods. Overall, the variation trends in the three K types are the same, presenting an obvious diurnal variation pattern. With the increase in radiation and temperature, the air turbulence becomes strong, and the three K types are increased. Around noon, the maximum K appears with smooth changes. It starts to decrease in the later afternoon. However, large differences exist in the three K values. The K value determined by the AG method (K_{AG}) is the largest, and the K calculated with the MBR method (K_{MBR}) is the smallest.

The K_{AGEC} value is between those of K_{MBR} and K_{AG}, and the variables for calculating K_{AGEC} are measured by the EC technique. It can therefore be considered the most appropriate, as validated by comparing its results with those of the EC O_3 flux (see section 3.3). The 30-min averaged K_{AG} and K_{MBR} are compared with K_{AGEC} in Fig. 2. Based on the scatterplot, coefficient of determination (R^2), and significance level, it is clear that the correlation between K_{MBR} and K_{AGEC} is better than that between K_{AG} and K_{AGEC}. Based on the linear regression equations, K_{MBR} is approximately 0.08 m s^{-1} lower than the K_{AGEC} in value, while the K_{AG} is larger than the K_{AGEC} overall. The difference becomes small when K is large. The mean values of K_{AGEC}, K_{MBR}, and K_{AG} are 0.20, 0.12, and 0.25, respectively. K_{MBR} is 40% lower and K_{AG} is 25% higher than K_{AGEC}.

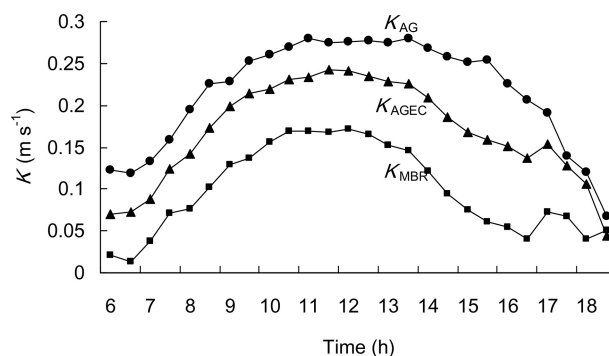The differences in the exchange coefficients are

Fig. 1. Diurnal variations of the K calculated by the MBR, AGEC and AG methods.
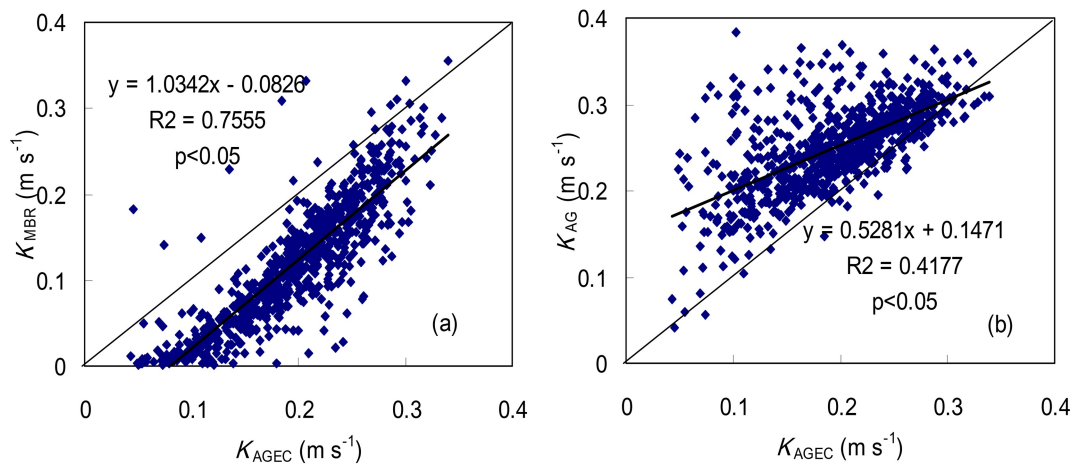
Fig. 2. Comparison of the 30-min K computed with the MBR, AGEC and AG methods.

affected by their calculation equations and the accuracy of each variable measurement. The large differences in the K values show that there were systematic errors in determining K with the different methods (see Fig.2). For K_{MBR}, the error sources include the H and temperature gradient measurements. Wilson et al. (2002) evaluated the energy balance closure of 22 sites in FLUXNET and concluded that a general lack of closure existed at most sites, with a mean imbalance in the order of 20% in most conditions. The sum of the measured H and LE (latent heat flux) with the EC method, $(H + LE)_{EC}$, is smaller than the difference in net radiation (R_n) and soil heat flux (G) $(R_n–G)$. This may imply that the H measured with EC might be underestimated, leading to the underestimation of K_{MBR}. Additionally, the error in the temperature gradient is dependent on the sensors' performance. Although the best precision that the temperature sensors can reach is ±0.055°C, as the two temperature sensors were not exchanged periodically, a radiation shield could also result in a certain systematic bias in the temperature at the two levels (Loubet et al., 2013). To eliminate the systematic error of two temperature sensors, using thermocouples rather than the routine temperature sensors may be a good choice. It would be better if two temperature sensors could be exchanged regularly.

The sources of error and uncertainty in K_{AG} come from the wind speed measurements, estimations of d, parameters of stability correction functions, etc. Wind speeds were measured with two new 2D sonic anemometers. The precision is ±0.1 m s⁻¹ or 2% of the readings, and the initial wind speed is 0.01 m s⁻¹ (according to the manual). We can consider the accuracy to be sufficiently high and the random error to be very limited. These assumptions would ensure that the wind speed gradient is reliable. Improper stability correction functions in Eq. (2) might also be error sources. The commonly used universal models and parameters of the functions are usually based on previous literature that utilized empirical equations obtained at a specific site and in a specific condition. Different researchers have presented different stability correction models and parameters (Foken, 2006; Song et al., 2010).

The error and uncertainty of zero-plane displacement (d) are dependent on the estimation method and parameters (Loubet et al., 2013). The commonly used method is simply estimated by the plant height (h_c) being multiplied by a constant (usually in the range of 0.6–0.8). The second method is inversely derived from the flux–gradient relationships, and the scalar flux can utilize the EC measurements. The third method is estimated by linearly fitting the wind speed profiles $U(z)$ and $\ln(z–d)$, making the root-mean-square error of the wind speed minimal in neutral conditions or making some corrections under non-neutral conditions. In this study, it was calculated as $d = 0.67h_c$. To validate whether this is suitable, we compared the u^* calculated by the third method (u^*_{AG}) and the u^* measured with the EC technique (u^*_{EC}), respectively. As seen in Fig. 3, the correlation is very good, with a slope of 0.99 and an R^2 of 0.8, indicating that the estimated d has no systematic bias.

3.2. O₃ concentration gradient

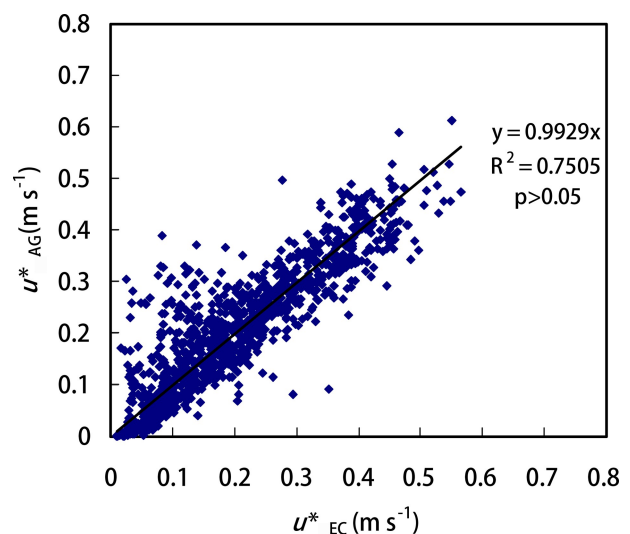Figure 4 shows the frequency distribution of the O₃ gradi-

Fig. 3. Comparison of u^* measured with the EC technique and AG method.

ent in the daytime during the observation period. Most gradients are distributed in the range between −6 μg m^{-3} and 0 μg m^{-3}, and the median of the gradient is −3 μg m^{-3}. As the two-level O$_3$ concentrations were measured with the same analyzer, the systematic error caused by the analyzers can be ignored. However, the random error must still be considered. The uncertainty or relative error of the gradient depends on the magnitude of the real gradient that can be estimated by the ratio of the sampling errors ($\delta_{\Delta C_{O_3}}$) to the gradient ΔC_{O_3} (Wolff et al., 2010). According to the manual, its precision and accuracy are greater than 1.0 ppb (approximately 1.9 μg m^{-3}) or 2% of the reading, and its resolution is 0.1 ppb. This allows the small O$_3$ gradient to be detected, but it is difficult to quantitatively determine the uncertainty in the O$_3$ gradient. Nevertheless, a zero-gradient test could be used to roughly evaluate the precision and accuracy of the flux-gradient system. The larger the gradient (absolute value) is, the smaller the uncertainty of the gradient.

Figure 5 shows the mean diurnal variations of the O$_3$ concentration (average of two levels) and gradient during the entire observation period. The analyzer is a new product, and its precision can guarantee that the O$_3$ concentration is reliable. Compared to the ambient absolute concentration, the vertical O$_3$ gradient is very small within the ranges of several ppb. In the morning, the gradient shows increasingly larger trends. It is less than 2 μg m^{-3} in the early morning (before 0900 LST), implying that there may be large uncertainty during this period. The change in the mean gradient is
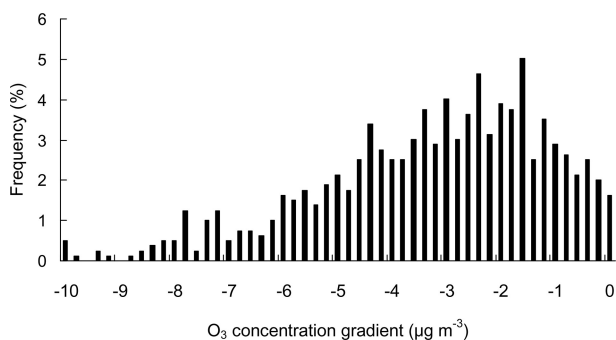

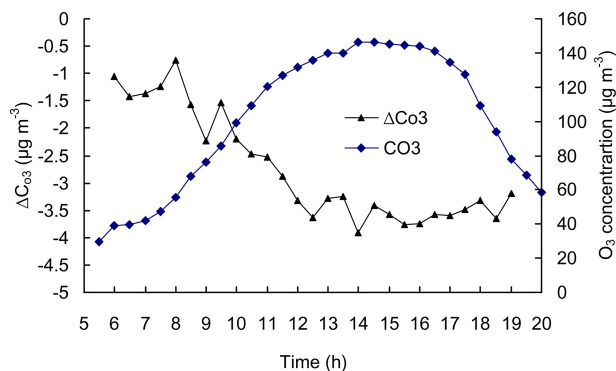**Fig. 4**. Frequency distribution of the O$_3$ concentration gradient.

Fig. 5. Mean diurnal variations of the O$_3$ concentration (average of two levels) and gradients during the entire observation period.

relatively stable in the afternoon, with a mean gradient of 3.6 μg m^{-3}, starting to decrease after 1900 LST.

In general, the negative effects of O$_3$ on crops happen in the daytime and during high concentration conditions (Pleijel et al., 2007; Feng et al., 2015). This can be reflected by O$_3$ concentration–based assessing indexes (Dingenen et al., 2009), such as M7 [the 7-h (0900–1600 LST) mean O$_3$ concentration] and AOT40 (the accumulated hourly O$_3$ concentration above a 40 ppbV threshold). The mean gradient was more than 2.4 μg m^{-3} in the later morning and afternoon at high O$_3$ concentrations (Fig. 5), implying that the uncertainty of the gradient is relatively small during the times that O$_3$ is affecting the ecosystem.

The accuracy of the O$_3$ gradient is a key variable for the O$_3$ flux measured with gradient methods. It depends on not only the analyzer's performance but also the measurement and calculation methods. For example, the number of measuring heights is a source of uncertainty for the gradient. According to AG theory, the flux is proportional to the concentration changes with height. For only the two-level measurements, a few random errors in the O$_3$ concentration could result in a large bias in the O$_3$ gradient. Hence, measuring the concentration profiles at more heights would filter or smooth out the random error, and the gradient would be more stable.

Besides the number of measuring heights, it is noteworthy that the proper calculation method is very important for reducing bias in the O$_3$ gradient. In this study, the two-level O$_3$ concentrations were measured alternately (in 5-min intervals) with one analyzer, in which there exists a measuring order issue (i.e., which 5-min O$_3$ concentration level is measured first during a 30-min period). A simple average of each of the O$_3$ concentration levels might produce certain errors without considering the measuring order. Table 1 presents an example of 30-min averaged O$_3$ mix ratio gradients with two calculation methods. In method I, the upper and lower 30-min O$_3$ concentrations are the simple re-average of three 5-min measurements. As shown in Table 1, the upper concentrations were measured during 1000–1005 LST, 1010–1015 LST, and 1020–1025 LST on 21 August 2017. The lower concentration measurements were taken during 1005–1010 LST, 1015–1020 LST, and 1025–1030 LST on 21 August 2017. In method II, the gaps were first filled with the averages before and after the 5-min measured O$_3$ concentrations, and there were six 5-min data points for each height, including three measured and three gap-filled data points. The gradient was then calculated as the difference between the two-height O$_3$ concentrations.

It is clear that there are large differences in the O$_3$ gradients determined with the two methods (see ΔC1 and ΔC2 in Table 1). To demonstrate that method II is better than method I, we calculated the gradient of an offset of 5 min (i.e., 1005–1035 LST), in which the measuring order is changed. With method I, the O$_3$ gradients of 1000–1030 LST (−2.30 ppb) and 1005–1035 LST (0.15 ppb) are largely variable and even result in a change of sign. However, the variation in the gradients of 1000–1030 LST and 1005–

Table 1. An example of a comparison of different O$_3$ mix ratio gradient calculation methods.

	Start Time (LST)						
	1000	1005	1010	1015	1020	1025	1030
C$_{O_3}$_upper (5 min, ppb)	58.66*	61.78	63.83*	65.87	65.99*	66.10	66.19*
C$_{O_3}$_lower (5 min, ppb)	57.77	60.78*	63.79	64.54*	65.28	65.21*	65.14
Mean1_upper (30 min)	64.58**	–	–	64.58***	–	–	–
Mean1_lower (30 min)	62.28**	–	–	64.74***	–	–	–
Mean2_upper (30 min)	63.70**	–	–	64.96***	–	–	–
Mean2_lower (30 min)	62.89**	–	–	64.12***	–	–	–
ΔC1 (Lower − upper)	−2.30**	–	–	0.15***	–	–	–
ΔC2 (Lower − upper)	−0.81**	–	–	−0.84***	–	–	–

Notes: *no measurements, filled with the average of the measurements before and after 5 min; **averages of 1000–1030 LST; ***averages of 1005–1035 LST. Mean1 (Method I) is the average of real measurements during a 30-min period with three data points; Mean2 (Method II) is the average of measurements and gap-filled data during a 30-min period with six data points. ΔC1 and ΔC2 are the differences in the lower and upper O$_3$ concentrations that are calculated with Mean1 and Mean2.

1035 LST calculated with method II is very small (−0.81 ppb and −0.84 ppb).

Figure 6 shows the diurnal variations of O$_3$ gradients calculated with two methods and time ranges on 15 August 2017. In method I, the difference of two 30-min averaged O$_3$ gradients during different time ranges (5-min offset) is very large sometimes (see the two solid lines in Fig. 6). However, the difference with method II is obviously small (see the two dashed lines in Fig. 6). Even so, the difference means that there was still some uncertainty in the O$_3$ gradient calculated with method II.

The main reason for this phenomenon is that the concentration changes in 5 min, and the O$_3$ gradient is on the same order of magnitude (maximum several ppb). If the measuring time is not synchronous, the gradient would be affected by the changing trend of the O$_3$ concentration. To ensure that both the upper and lower intakes measure the same air eddy, setting a quick switching time (e.g. ~1 min) may eliminate the phenomenon and improve the performance of the gradient system. Of course, if possible, the use of two analyzers and periodically exchanging the sample position to measure the O$_3$ concentrations at two heights is better than using one analyzer to cyclically measure them (Meyers et al.,
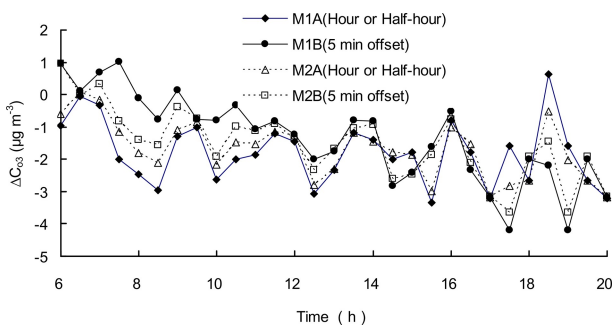

Fig. 6. Diurnal variations of 30-min averaged O$_3$ gradients calculated with two methods and time ranges on 15 August 2017. M1A: Method I and start times are on the hour or half-hour; M1B: Method I but start times are 5-min delayed; M2A: Method II and start times are on the hour or half-hour; M2B: Method II but start times are 5-min delayed.

1996). This not only removes the systematic bias from the two analyzers but can also eliminate the errors caused by asynchronous sampling.

3.3. Comparison of O$_3$ fluxes measured with the EC and different gradient methods

Figure 7 presents the mean diurnal variations of the O$_3$ fluxes with different methods. The disparities in the O$_3$ fluxes with different methods were small in the morning and large in the afternoon. This is primarily because the gradient was relatively large in the afternoon (see Fig. 5). As the analyzer's random error is relatively small and stable, its effect on the O$_3$ flux will decrease at a large gradient. Relatively, the O$_3$ flux calculated by the AGEC method ($F_{O_3\_AGEC}$) is closest to $F_{O_3\_EC}$. The MBR O$_3$ flux ($F_{O_3\_MBR}$) is lower than $F_{O_3\_EC}$, and the AG O$_3$ flux ($F_{O_3\_AG}$) in the afternoon is about twice as large as $F_{O_3\_EC}$.

Figure 8 shows comparisons of daytime O$_3$ fluxes calculated by the EC method ($F_{O_3\_EC}$) and the F_{O_3} calculated by different gradient methods. Overall, the correlations between $F_{O_3\_EC}$ and O$_3$ fluxes with different gradient methods are not good. To analyze the relationships between $F_{O_3\_EC}$ and the fluxes from different gradient methods, two types of linear regression equations were calculated. Type 1 is the general linear regression equation, and type 2 is the linear equation with the intercept phased to zero, reflecting the relationships between the two mean fluxes. Relatively, the gradient method's O$_3$ flux with AGEC is the best, with the largest R^2 (0.1845), and the slope of the type 2 linear regression curve is closest to the 1:1 line (Fig. 8b). The low correlations show that the gradient O$_3$ fluxes were not very reliable.

A few previous studies compared the gradient O$_3$ flux with that of the EC technique and found that the results varied. Muller et al. (2009) found that the O$_3$ flux determined by the gradient method was larger than that of the EC technique at a grassland area. The transfer coefficient was derived by the wind speed gradient and EC momentum flux. It also showed a very large comparison scatterplot, with a slope of 1.19 and a poor R^2 (0.15). The O$_3$ flux with the AGEC method was similar to the results presented by
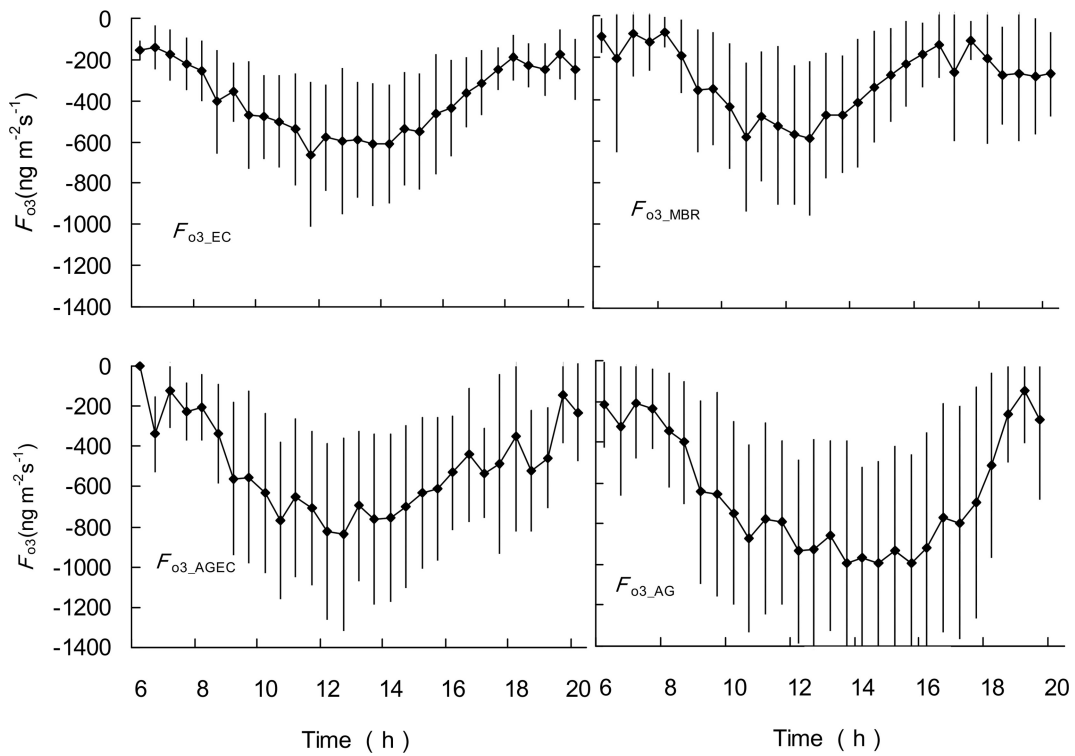
Fig. 7. Mean diurnal variations of the O_3 fluxes estimated by different methods. The top and bottom of the vertical lines represent the mean ± std.
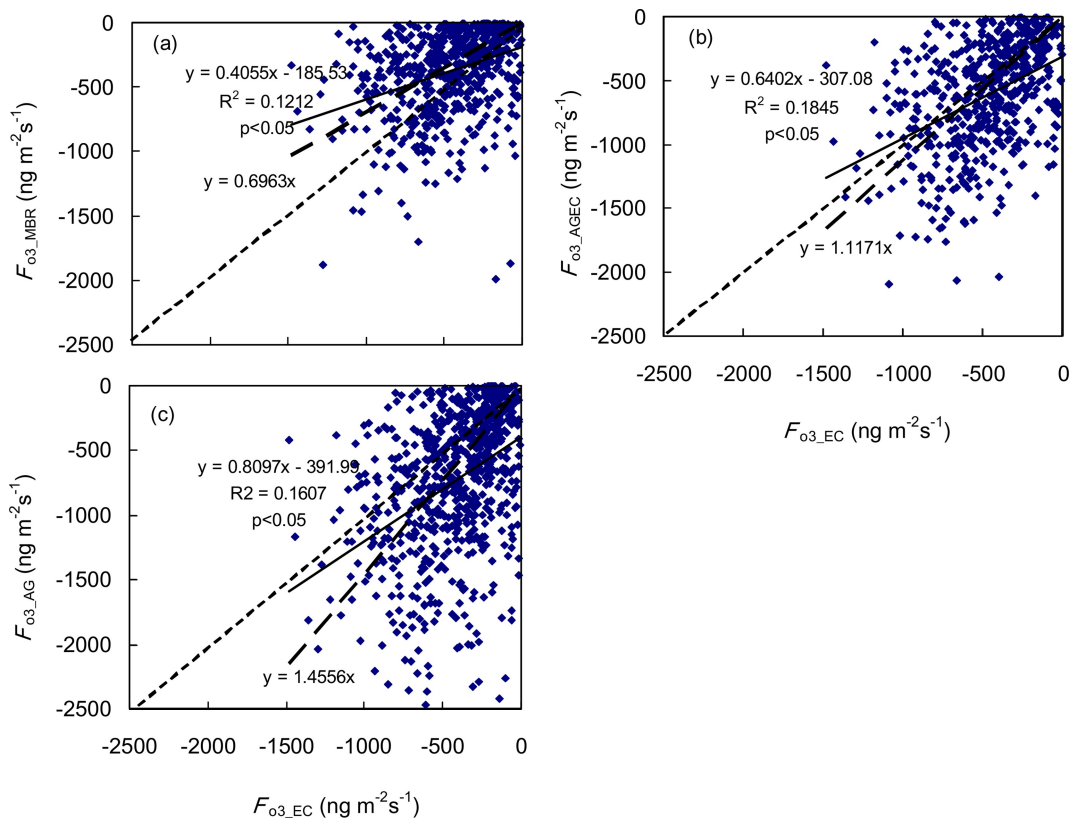

Fig. 8. Comparisons of 30-min O_3 fluxes estimated by different gradient methods and the EC method's flux.

Muller et al. (2009). Loubet et al. (2013) compared the O_3 fluxes and deposition velocities (V_d) with AG methods and the EC technique over a maize field and showed that the AG method had a roughly 40% larger V_d than the EC technique. In this study, the AG O_3 flux was calculated from the product of u^* (calculated by the wind speed gradient with a

stability correction) by a concentration scaling parameter $C_{O_3}^*$ (determined by the O$_3$ concentration gradient with a stability correction). The F_{O_3} calculated with the AG method is close to these results. Keronen et al. (2003) found that the V_d values determined by the AG method and EC technique generally agreed well in a Nordic pine forest, as did Stella et al. (2012) over bare soil in Paris. Droppo (1985) found that the V_d determined with the MBR method was close to that of the EC method at a Northeastern U.S. grassland site. Although the O$_3$ flux with the AGEC method approaches that of the EC method in these results, the agreement is not very good.

The errors of the gradient method's fluxes come from the joint effects of the exchange coefficient and gradient. The theoretical basis of the gradient method is MOST, but it is limited to the homogeneous surface layer (or constant-flux layer) above the roughness sub-layer, and a range of $|z/L| \leqslant 1 \sim 2$ (Foken, 2006). The large discrepancy among the O$_3$ fluxes with different methods may be related to the non-ideal conditions. For example, the sensors' heights were not elevated enough, and the turbulent intensity was not always strong enough. Rinne et al. (2000) summarized the sources of uncertainty with AG methods for hydrocarbon flux measurements and presented the error estimate of gradient measurements, turbulent exchange coefficients, and parameterizations. The uncertainty caused by the gradient measurement was the largest. Loubet et al. (2013) also analyzed the potential errors in the AG method. They included the non-stationarity of the concentration changes, temperature errors caused by shields, roughness sub-layer correction issues, uncertainty in the displacement height estimation, etc. Based on this error source analysis, the most important error source was determined to be the gradient measurement. Decreasing the uncertainty in the O$_3$ gradient is the key to more accurately estimating the O$_3$ flux for gradient methods. Increasing the number of analyzers and measuring levels might reduce the errors in the O$_3$ gradient. The gradient calculated using only the two-level O$_3$ concentrations can easily produce random errors.

4. Conclusions

In this study, we evaluated the performance of different gradient methods for the O$_3$ flux measurement by comparing them with the EC O$_3$ flux. The accuracy and precision of the gradient method O$_3$ flux rely on the measurement and calculation methods of the exchange coefficients and concentration gradients. The following conclusions can be drawn from our results.

The exchange coefficients calculated with different methods showed similar diurnal variation patterns. The coefficient calculated using the EC measurements (K_{AGEC}) is the most accurate. On average, the coefficient computed by the MBR method (K_{MBR}) is 40% lower than K_{AGEC}, and the coefficient based on the AG method (K_{AG}) is 25% higher than K_{AGEC}.

Because of the small concentration difference in two layers over the maize field, the bias and uncertainty of the O$_3$ gradient mainly depend on the analyzer's precision. Meanwhile, measurement and calculation methods are also important sources of error for the O$_3$ gradient and should be paid attention. When using one analyzer to cyclically measure the two-level O$_3$ concentrations, the effect of the fast O$_3$ concentration changes on the O$_3$ gradient must be eliminated. Using two analyzers and periodically exchanging the sampling position to measure two-height O$_3$ concentrations is a better option.

By comparing the gradient's O$_3$ fluxes with that of the EC technique, we found that the correlations between the $F_{O_3\_EC}$ and F_{O_3} with gradient methods are not very good. The accuracy of the gradient method is dependent on the exchange coefficient method, and the precision is related to the quality of the O$_3$ gradient measurement. On average, the gradient method O$_3$ fluxes with the AG, AGEC, and MBR methods were 30.4% lower, 11.7% higher, and 45.6% higher than $F_{O_3\_EC}$, respectively. The O$_3$ fluxes determined with the AGEC method are the closest to that determined with the EC technique.

REFERENCES

Baldocchi, D. D., 2003: Assessing the eddy covariance technique for evaluating carbon dioxide exchange rates of ecosystems: Past, present and future. *Global Change Biology*, **9**, 479−492, https://doi.org/10.1046/j.1365-2486.2003.00629.x.

Baldocchi, D. D., and T. Meyers, 1998: On using eco-physiological, micrometeorological and biogeochemical theory to evaluate carbon dioxide, water vapor and trace gas fluxes over vegetation: A perspective. *Agricultural and Forest Meteorology*, **90**, 1−25, https://doi.org/10.1016/S0168-1923(97)00072-5.

Bocquet, F., D. Helmig, B. A. Van Dam, and C. W. Fairall, 2011: Evaluation of the flux gradient technique for measurement of ozone surface fluxes over snowpack at Summit, Greenland. *Atmospheric Measurement Techniques*, **4**, 2305−2321, https://doi.org/10.5194/amt-4-2305-2011.

Businger, J. A., J. C. Wyngaard, Y. Izumi, and E. F. Bradley, 1971: Flux-profile relationships in the atmospheric surface layer. *J. Atmos. Sci.*, **28**, 181−189, https://doi.org/10.1175/1520-0469(1971)028<0181:FPRITA>2.0.CO;2.

Cape, J. N., 2008: Surface ozone concentrations and ecosystem health: Past trends and a guide to future projections. *Science of The Total Environment*, **400**, 257−269, https://doi.org/10.1016/j.scitotenv.2008.06.025.

Droppo, J. G., 1985: Concurrent measurements of ozone dry deposition using eddy correlation and profile flux methods. *J. Geophys. Res. Atmos.*, **90**, 2111−2118, https://doi.org/10.1029/JD090iD01p02111.

Feng, Z. Z., E. Z. Hu, X. K. Wang, L. J. Jiang, and X. J. Liu, 2015: Ground-level O$_3$ pollution and its impacts on food

crops in China: A review. *Environmental Pollution*, **199**, 42−48, https://doi.org/10.1016/j.envpol.2015.01.016.

Foken, T., 2006: 50 years of the Monin-Obukhov similarity theory. *Bound.-Layer Meteorol.*, **119**, 431−447, https://doi.org/10.1007/s10546-006-9048-6.

Fu, Y., H. Liao, and Y. Yang, 2019: Interannual and decadal changes in tropospheric ozone in China and the associated chemistry-climate interactions: A review. *Adv. Atmos. Sci.*, **36**(9), 975−993, https://doi.org/10.1007/s00376-019-8216-9.

Grünhage, L., H. D. Haenel, and H. J. Jäger, 2000: The exchange of ozone between vegetation and atmosphere: Micrometeorological measurement techniques and models. *Environmental Pollution*, **109**, 373−392, https://doi.org/10.1016/S0269-7491(00)00041-5.

Güsten, H., G. Heinrich, R. W. H. Schmidt, and U. Schurath, 1992: A novel ozone sensor for direct eddy flux measurements. *Journal of Atmospheric Chemistry*, **14**, 73−84, https://doi.org/10.1007/BF00115224.

Ibrom, A., E. Dellwik, H. Flyvbjerg, N. O. Jensen, and K. Pilegaard, 2007: Strong low-pass filtering effects on water vapour flux measurements with closed-path eddy correlation systems. *Agricultural and Forest Meteorology*, **147**, 140−156, https://doi.org/10.1016/j.agrformet.2007.07.007.

Karlsson, P. E., and Coauthors, 2007: Risk assessments for forest trees: the performance of the ozone flux versus the AOT concepts. *Environmental Pollution*, **146**, 608−616, https://doi.org/10.1016/j.envpol.2006.06.012.

Keronen, P., and Coauthors, 2003: Ozone flux measurements over a scots pine forest using eddy covariance method: Performance evaluation and comparison with flux-profile method. *Boreal Environment Research*, **8**, 425−443.

Krzyscin, J., P. Krizan, and J. Jarosławski, 2007: Long-term changes in the tropospheric column ozone from the ozone soundings over Europe. *Atmos. Environ.*, **41**, 606−616, https://doi.org/10.1016/j.atmosenv.2006.08.026.

Loubet, B., and Coauthors, 2013: Investigating discrepancies in heat, CO_2 fluxes and O_3 deposition velocity over maize as measured by the eddy-covariance and the aerodynamic gradient methods. *Agricultural and Forest Meteorology*, **169**, 35−50, https://doi.org/10.1016/j.agrformet.2012.09.010.

Massman, W. J., 2004: Toward an ozone standard to protect vegetation based on effective dose: A review of deposition resistances and a possible metric. *Atmos. Environ.*, **38**, 2323−2337, https://doi.org/10.1016/j.atmosenv.2003.09.079.

Massman, W. J., and X. Lee, 2002: Eddy covariance flux corrections and uncertainties in long-term studies of carbon and energy exchanges. *Agricultural and Forest Meteorology*, **113**, 121−144, https://doi.org/10.1016/S0168-1923(02)00105-3.

Mayer, J. C., A. Bargsten, U. Rummel, F. X. Meixner, and T. Foken, 2011: Distributed Modified Bowen Ratio method for surface layer fluxes of reactive and non-reactive trace gases. *Agricultural and Forest Meteorology*, **151**, 655−668, https://doi.org/10.1016/j.agrformet.2010.10.001.

Meyers, T. P., M. E. Hall, S. E. Lindberg, and K. Kim, 1996: Use of the modified bowen-ratio technique to measure fluxes of trace gases. *Atmos. Environ.*, **30**, 3321−3329, https://doi.org/10.1016/1352-2310(96)00082-9.

Mills, G., and Coauthors, 2011: New stomatal flux-based critical levels for ozone effects on vegetation. *Atmos. Environ.*, **45**, 5064−5068, https://doi.org/10.1016/j.atmosenv.2011.06.009.

Moncrieff, J. B., and Coauthors, 1997: A system to measure sur-

face fluxes of momentum, sensible heat, water vapour and carbon dioxide. *J. Hydrol.*, **188−189**, 589−611, https://doi.org/10.1016/S0022-1694(96)03194-0.

Muller, J. B. A., M. Coyle, D. Fowler, M. W. Gallagher, E. G. Nemitz, and C. J. Percival, 2009: Comparison of ozone fluxes over grassland by gradient and eddy covariance technique. *Atmospheric Science Letters*, **10**, 164−169, https://doi.org/10.1002/asl.226.

Muller, J. B. A., C. J. Percival, M. W. Gallagher, D. Fowler, M. Coyle, and E. Nemitz, 2010: Sources of uncertainty in eddy covariance ozone flux measurements made by dry chemiluminescence fast response analysers. *Atmospheric Measurement Techniques*, **3**, 163−176, https://doi.org/10.5194/amt-3-163-2010.

Musselman, R. C., A. S. Lefohn, W. J. Massman, and R. L. Heath, 2006: A critical review and analysis of the use of exposure- and flux-based ozone indices for predicting vegetation effects. *Atmos. Environ.*, **40**, 1869−1888, https://doi.org/10.1016/j.atmosenv.2005.10.064.

Paoletti, E., and W. J. Manning, 2007: Toward a biologically significant and usable standard for ozone that will also protect plants. *Environmental Pollution*, **150**, 85−95, https://doi.org/10.1016/j.envpol.2007.06.037.

Paulson, C. A., 1970: The mathematical representation of wind speed and temperature profiles in the unstable atmospheric surface layer. *J. Appl. Meteorol.*, **9**, 857−861, https://doi.org/10.1175/1520-0450(1970)009<0857:TMROWS>2.0.CO;2.

Pleijel, H., H. Danielsson, L. Emberson, M. R. Ashmore, and G. Mills, 2007: Ozone risk assessment for agricultural crops in Europe: Further development of stomatal flux and flux-response relationships for European wheat and potato. *Atmos. Environ.*, **41**, 3022−3040, https://doi.org/10.1016/j.atmosenv.2006.12.002.

Rinne, J., J.-P. Tuovinen, T. Laurila, H. Hakola, M. Aurela, and H. Hypén, 2000: Measurements of hydrocarbon fluxes by a gradient method above a northern boreal forest. *Agricultural and Forest Meteorology*, **102**, 25−37, https://doi.org/10.1016/S0168-1923(00)00088-5.

Song, X. Z, H. S. Zhang, J. Y. Chen, and S. U. Park, 2010: Flux-gradient relationships in the atmospheric surface layer over the Gobi Desert in China. *Bound.-Layer Meteorol.*, **134**, 487−498, https://doi.org/10.1007/s10546-009-9457-4.

Stella, P., and Coauthors, 2012: Comparison of methods for the determination of NO-O3-NO2 fluxes and chemical interactions over a bare soil. *Atmospheric Measurement Techniques*, **5**, 1241−1257, https://doi.org/10.5194/amt-5-1241-2012.

van Dingenen, R., F. J. Dentener, F. Raes, M. C. Krol, L. Emberson, and J. Cofala, 2009: The global impact of ozone on agricultural crop yields under current and future air quality legislation. *Atmos. Environ.*, **43**, 604−618, https://doi.org/10.1016/j.atmosenv.2008.10.033.

Walker, J. T., W. P. Robarge, Y. Wu, and T. P. Meyers, 2006: Measurement of bi-directional ammonia fluxes over soybean using the modified Bowen-ratio technique. *Agricultural and Forest Meteorology*, **138**, 54−68, https://doi.org/10.1016/j.agrformet.2006.03.011.

Webb, E. K., G. I. Pearman, and R. Leuning, 1980: Correction of flux measurements for density effects due to heat and water vapour transfer. *Quart. J. Roy. Meteorol. Soc.*, **106**, 85−100, https://doi.org/10.1002/qj.49710644707.

Wilczak, J. M., S. P. Oncley, and S. A. Stage, 2001: Sonic anemo-

meter tilt correction algorithms. *Bound.-Layer Meteorol.*, **99**, 127–150, https://doi.org/10.1023/A:1018966204465.

Wilson, K., and Coauthors, 2002: Energy balance closure at FLUXNET sites. *Agricultural and Forest Meteorology*, **113**, 223–243, https://doi.org/10.1016/S0168-1923(02)00109-0.

Wolff, V., I. Trebs, C. Ammann, and F. X. Meixner, 2010: Aerodynamic gradient measurements of the NH_3-HNO_3-NH_4NO_3 triad using a wet chemical instrument: an analysis of precision requirements and flux errors. *Atmospheric Measurement Techniques*, **3**, 187–208, https://doi.org/10.5194/amt-3-187-2010.

Wu, Z. Y., L. Zhang, X. M. Wang, and J. W. Munger, 2015: A modified micrometeorological gradient method for estimating O3 dry depositions over a forest canopy. *Atmospheric Chemistry and Physics*, **15**, 7487–7496, https://doi.org/10.5194/acp-15-7487-2015.

Zahn, A., J. Weppner, H. Widmann, K. Schlote-Holubek, B. Burger, T. Kühner, and H. Franke, 2012: A fast and precise chemiluminescence ozone detector for eddy flux and airborne application. *Atmospheric Measurement Techniques*, **5**, 363–375, https://doi.org/10.5194/amt-5-363-2012.

Zhu, Z. L., F. H. Zhao, L. Voss, L. K. Xu, X. M. Sun, G. R. Yu, and F. X. Meixner, 2015: The effects of different calibration and frequency response correction methods on eddy covariance ozone flux measured with a dry chemiluminescence analyzer. *Agricultural and Forest Meteorology*, **213**, 114–125, https://doi.org/10.1016/j.agrformet.2015.06.016.